

AR6 WGI Report – List of corrigenda to be implemented

The corrigenda listed below will be implemented in the Supp. Material during copy-editing.

CHAPTER 6 Supplementary Material

Document (Chapter, Annex, Supp. Mat...)	Section	Page :Line (based on the final pdf FGD version)	Detailed info on correction to make
6SM	6.SM.1		A bit more explanation has been provided for the calculation of emissions-based ERFs, in particular the scaling performed for aerosol forcings has been clarified. Tables showing the values plotted in Figure 6.12 are now included in the supplementary. The revised supplementary is uploaded on the DMS
6SM			Update the Data Table with omitted data citations for climate model data.
6SM	6.SM.1	3:26-28	<p>“The contribution from aerosol radiation interaction (ari) is calculated as the difference between the total ERF and ERFaci. Thus, the non-cloud adjustments are included as aerosol radiation interaction.”</p> <p>Is now “The contribution from aerosol radiation interactions (ari) is calculated as the difference between the total ERF and ERF due to cloud interactions (ERFaci). Thus, the non-cloud adjustments are included as aerosol radiation interaction. Because the total aerosol ERFari and ERFaci for 2014 based on AerChemMIP models are more negative and less negative, respectively, compared to that assessed in Chapter 7, the individual aerosol ERFs are scaled relative to total aerosol ERFs in Chapter 7 Section 7.3.3.4 to account for this bias. For BC, the cloud effect is assumed to scale with the aerosol ERFari rather than the aerosol ERFaci.”</p> <p>For clarification</p>
6SM	6.SM.1	3:33	“(i.e., from CH ₄ , CO, NMVOCs and halocarbons)” has been added for clarification
6SM	6.SM.1	3:41	“In Figure 6.22 and 6.24 we consider HFCs with lifetimes shorter than about 50 years (as reported by Hodnebrog et al., 2020): HFC-134a, HFC-32, HFC-125, HFC-143a, HFC-152a, HFC-227ea, HFC-245fa, HFC-365mfc, HFC-43-10mee.” has been added for clarification
6SM	6.SM.1	3:44	A table “Table 6.SM.1. Effective radiative forcing (ERF, in Wm ⁻²) by emitted components for the period 1750-2019 as shown in Figure 6.12.” has been added
6SM	6.SM.1	3:44	A Table “Table 6.SM.2. Changes in global mean surface air temperature (GSAT) due to emitted components for the period 1750-2019 as shown in Figure 6.12.” has been added
6SM	6.SM.2	3:49	“GSAT changes shown in Figure 6.12 are presented in Table 6.SM.2.” has been added
6SM	6.SM.1	11	In Table 6.SM.1: Row 1, Column 1: “Figure number / Table number / Chapter section (for calculations)” replace with “Figure number”
6SM	6.SM.1	11	In Table 6.SM.1: Add new column 9 at the end “Notes”

6SM	6.SM.1	11	In Table 6.SM.1: Row 2, Column 4: Add “CMIP6 Data Release (data only) July 26, 2016 for CEDS »
6SM	6.SM.1	11	In Table 6.SM.1: Row 2, Column 7: Add “ https://github.com/JGCRI/CEDS/ ”
6SM	6.SM.1	11	In Table 6.SM.1: Row 3, Column 8: “(Young et al., 2013, 2018; DuplicateGriffiths et al., 2020) ” replace with “(Griffiths et al., 2020; Young et al., 2013, 2018)”
6SM	6.SM.1	11	In Table 6.SM.1: Row 3, Column 5: public ” replace with “ https://esgf.llnl.gov/LICENSE.html ”
6SM	6.SM.1	14	In Table 6.SM.1: Row 2, Column 7: “Code to be placed in https://github.com/IPCC-WG1 ” replace with “ https://github.com/IPCC-WG1/Chapter-6 ”
6SM	6.SM.1	14	In Table 6.SM.1: Row 3, Column 5: add “ https://esgf.llnl.gov/LICENSE.html ”
6SM	6.SM.1	14	In Table 6.SM.1: Row 4, Column 5: add “ https://esgf.llnl.gov/LICENSE.html ”
6SM	6.SM.1	15	In Table 6.SM.1: Row 5, Column 5: add “ https://esgf.llnl.gov/LICENSE.html ”
6SM	6.SM.1	15	In Table 6.SM.1: Row 6, Column 8: Delete “(Myhre et al., 2013)”
6SM	6.SM.1	15	In Table 6.SM.1: Row 7, Column 7: “Code to be placed in https://github.com/IPCC-WG1/TBD ” replace with “ https://github.com/IPCC-WG1/Chapter-6 ”
6SM	6.SM.1	16	In Table 6.SM.1: Row 6, Column 7: delete “Code to be placed in https://github.com/IPCC-WG1/TBD ”
6SM	6.SM.1	16	In Table 6.SM.1: Row 6, Column 5: public ” replace with “ https://esgf.llnl.gov/LICENSE.html ”
6SM	6.SM.1	16	In Table 6.SM.1: Row 6, Column 8: Delete “(Myhre et al., 2013)”
6SM	6.SM.1	17	In Table 6.SM.1: Row 7, Column 2: “CMIP6” replace with “Figure 6.12 code”
6SM	6.SM.1	17	In Table 6.SM.1: Row 7, Column 3: “Input dataset” replace with “Code”
6SM	6.SM.1	17	In Table 6.SM.1: Row 7, Column 6: Delete “Eyring et al. 2016”
6SM	6.SM.1	17	In Table 6.SM.1: Row 7, Column 7: Delete “ https://esgf-node.llnl.gov/search/cmip6/ ” Code to be placed in https://github.com/IPCC-WG1/TBD ”
6SM	6.SM.1	17	In Table 6.SM.1: Row 7, Column 8: “(Ghan, 2013; DuplicateThornhill et al., 2021) ” replace with “(Ghan, 2013; Joos et al., 2013; Stevenson et al., 2013; Thornhill et al., 2021).”
6SM	6.SM.1	17	In Table 6.SM.1: Row 7, Column 9: Add “See IPCC AR6 WG1 6.SM.1, 6.SM.2 for details and 7.SM.1”
6SM	6.SM.1	17	In Table 6.SM.1: Row 8, Column 5: add “ https://esgf.llnl.gov/LICENSE.html ”
6SM	6.SM.1	17	In Table 6.SM.1: Row 8, Column 7: Delete “Code to be placed in https://github.com/IPCC-WG1/TBD ”
6SM	6.SM.1	17	In Table 6.SM.1: Row 9, Column 5: add “ https://esgf.llnl.gov/LICENSE.html ”
6SM	6.SM.1	17	In Table 6.SM.1: Row 9, Column 7: Delete “Code to be placed in https://github.com/IPCC-WG1/TBD ”
6SM	6.SM.1	18	In Table 6.SM.1: Row 7, Column 2: “ScenarioMIP experiments ssp370SST, ssp370pdSST Mole fraction of ozone ” replace with “Figure 6.15 code”
6SM	6.SM.1	18	In Table 6.SM.1: Row 7, Column 3: “Input dataset OUTPUT DATA FREQUENCY” replace with “Code”
6SM	6.SM.1	18	In Table 6.SM.1: Row 7, Column 4 5 6 7: Delete all
6SM	6.SM.1	18	In Table 6.SM.1: Row 7, Column 9: Add “See IPCC AR6 WG1 6.SM.1, 6.SM.2 for details”

6SM	6.SM.1	18	In Table 6.SM.1: Row 8, Column 2: "CMIP6, ScenarioMIP experiments ssp370SST, ssp370pdSST " replace with "Community Emissions Data System (CEDS) for Historical Emissions GAINS model Figure 6.16 code"
6SM	6.SM.1	18	In Table 6.SM.1: Row 8, Column 3: "Input dataset OUTPU T DATA FREQU ENCY " replace with "Input Dataset Input Dataset Code"
6SM	6.SM.1	18	In Table 6.SM.1: Row 8, Column 4: "CMIP6 models GFDL-ESM4, GISS-E2-1-G, MRI-ESM2-0 and UKESM1-0-LL " replace with "CMIP6 Data Release (data only) July 26, 2016 for CEDS ECLIPSE version 6b"
6SM	6.SM.1	18	In Table 6.SM.1: Row 8, Column 5: "public " replace with "Open Source"
6SM	6.SM.1	18	In Table 6.SM.1: Row 8, Column 6: "(Eyring et al., 2016; O'Neill et al., 2016) " replace with "(Klimont et al., 2017) (Lee et al., 2020; Purohit et al., 2020; van Marle et al., 2017)"
6SM	6.SM.1	18	In Table 6.SM.1: Row 8, Column 7: " https://esgf-node.llnl.gov/search/cmip6/ " replace with " http://www.globalchange.umd.edu/ceds/ https://github.com/JGCRI/CEDS/ https://iiasa.ac.at/web/home/research/researchPrograms/air/Global_emissions.html "

6SM	6.SM.1	18	Figure 6.18	GEIA/AC CENT gridded emissions	Input dataset	public		http://geiacenter.org	(Lamarque et al., 2010)		
				Community Emissions Data System (CEDS) for Historical Emissions	Input dataset	Gmd-11-369-2018-supplement input4MIPs.CMIP6.CMIP.VUA.VUA-CMIP-BB4CMIP6-1-2 CMIP6 Data Release (data only) July 26, 2016 for CEDS	public	(Hoesly et al., 2018; van Marle et al., 2017)	http://www.globalchange.umd.edu/ceds/ https://github.com/JGCR1/CEDS/ http://esgf-node.llnl.gov/search/input4mips/		
				EDGAR 5.0	Input dataset		public	(Crippa et al., 2019b, 2020)	https://edgar.jrc.ec.europa.eu/ , https://edgar.jrc.ec.europa.eu/dataset_ap50		
				ECLIPSE	Input dataset	ECLIPSE_v5a	public	(Klimont et al., 2017)(Stohl et al., 2015)	https://iiasa.ac.at/web/home/research/researchPrograms/air/Global_emissions.html https://iiasa.ac.at/web/home/research/researchPrograms/air/ECLIPSEv5a.html		
				SSP Database (Shared)	Input dataset	SSP_CMIP6_201811.csv.zip	public	(Gidden et al., 2019; Riahi et al.,	https://tntcat.iiasa.ac.at/SspDb/dsd		

			Socioeconomic Pathways) - Version 2.0				2017; Rogelj et al., 2018)			
In Table 6.SM.1: Row 8, Column 9: Add "See IPCC AR6 WG1 6.SM.4 for details"										
6SM	6.SM.1	19		In Table 6.SM.1: Row 1, Column 2: "CMIP6, ScenarioMIP Mole fraction of ozone" replace with "TM5-FASST model Community Emissions Data System (CEDS) for Historical Emissions CAMS global reanalysis (EAC4) Figure 6.17 code"						
6SM	6.SM.1	19		In Table 6.SM.1: Row 1, Column 3: "Input dataset intermediate data " replace with "Input Dataset Input Dataset Code"						
6SM	6.SM.1	19		In Table 6.SM.1: Row 1, Column 4: "GFDL-ESM4, BCC-ESM1, CESM2-WACCM and UKESM1- 0-LL for ssp370, GFDL-ESM4, BCC-ESM1, and CESM2- WACCM for ssp370-lowNTCF, GFDL-ESM4 and UKESM1-0-LL for SSP1-2.6, SSP2-4.5 and SSP5- 8.5 " replace with "CMIP6 Data Release (data only) July 26, 2016 for CEDS"						
6SM	6.SM.1	19		In Table 6.SM.1: Row 1, Column 5: "public " replace with "Open Source https://apps.ecmwf.int/datasets/licences/copernicus/ "						
6SM	6.SM.1	19		In Table 6.SM.1: Row 1, Column 6: "(Eyring et al., 2016; O'Neill et al., 2016) " replace with "(Van Dingenen et al., 2018) (Inness et al., 2019)"						
6SM	6.SM.1	19		In Table 6.SM.1: Row 1, Column 7: " https://esgf-node.llnl.gov/search/cmip6/ " replace with " http://www.globalchange.umd.edu/ceds/ https://github.com/JGCRI/CEDS/ https://www.ecmwf.int/en/forecasts/dataset/cams-global-reanalysis "						
6SM	6.SM.1	19		In Table 6.SM.1: Row 1, Column 8: Add "(Hoesly et al., 2018)"						
6SM	6.SM.1	19		In Table 6.SM.1: Below the row "Figure 6.17" add a new row						
6SM	6.SM.1	19	In Table 6.SM.1: Below the row "Figure 6.18" add a new row							
			Figure 6.19	GEIA/ACCENT gridded emissions	Input dataset		public		http:// geiacenter.org	(Lamarque et al., 2010)
				Community Emissions Data System (CEDS) for Historical Emissions	Input dataset	Gmd-11-369-2018-supplement input4MIPs.CMIP6.CMIP	public	(Hoesly et al., 2018; van Marle et al., 2017)	http://www.globalchange.umd.edu/ceds/ https://github.com/JGCRI/CEDS/	

					.VUA.VUA-CMIP-BB4CMIP6-1-2 CMIP6 Data Release (data only) July 26, 2016 for CEDS			http://esgf-node.llnl.gov/search/input4mips/		
			SSP Database (Shared Socioeconomic Pathways) - Version 2.0,	Input dataset	SSP_CMIP6_201811.csv.zip	public	(Gidden et al., 2019; Riahi et al., 2017; Rogelj et al., 2018)	https://tntcat.iiasa.ac.at/SspDb/dsd		
			Representative Concentration Pathway (RCP) database	Input dataset	Direct from website	public	(van Vuuren et al., 2011)	https://tntcat.iiasa.ac.at/RcpDb/dsd		
			Figure 6.19 code	Code				https://github.com/gidden/ar6-wg1-ch6-emissions		
6SM	6.SM.1	23	In Table 6.SM.1: Below the row "Figure 6.25" add a new row							
			Figure 6.26	Shared Socio-Economic Pathway (SSP) database	Input dataset			(Gidden et al., 2019; Riahi et al., 2017; Rogelj et al., 2018)	https://tntcat.iiasa.ac.at/SspDb/dsd	(Rao et al., 2017; Riahi et al., 2017)
Chapter 6 SM	6.SM.1	24	In Table 6.SM.1: Below the row "Figure 6.SM2" add a new row							
			Figure 6.SM.3	Community Emissions Data System (CEDS) for	Input dataset	CMIP6 Data Release (data only) July 26, 2016 for CEDS	Open Source		http://www.globalchange.umd.edu/ceds/ https://github.com/JGCRI/CEDS/	(Hoesly et al., 2018)

				Historical Emissions										
--	--	--	--	-------------------------	--	--	--	--	--	--	--	--	--	--

Chapter 6: Short-lived Climate Forces Supplementary Material

Coordinating Lead Authors:

Vaishali Naik (United States of America), Sophie Szopa (France)

Lead Authors:

Bhupesh Adhikary (Nepal), Paulo Artaxo (Brazil), Terje Berntsen (Norway), William D. Collins (United States of America), Sandro Fuzzi (Italy), Laura Gallardo (Chile), Astrid Kiendler-Scharr (Germany/Austria), Zbigniew Klimont (Austria/Poland), Hong Liao (China), Nadine Unger (United Kingdom/United States of America), Prodromos Zanis (Greece)

Contributing Authors:

Wenche Aas (Norway), Dimitris Akritidis (Greece), Robert J. Allen (United States of America), Nicolas Bellouin (United Kingdom/France), Sophie Berger (France/Belgium), Sara M. Blichner (Norway), Josep G. Canadell (Australia), William Collins (United Kingdom), Owen R. Cooper (United States of America), Frank J. Dentener (EU/The Netherlands), Sarah Doherty (United States of America), Jean-Louis Dufresne (France), Sergio Henrique Faria (Spain/Brazil), Piers Forster (United Kingdom), Tzung-May Fu (China), Jan S. Fuglestvedt (Norway), John C. Fyfe (Canada), Aristeidis K. Georgoulias (Greece), Matthew J. Gidden (Austria/ United States of America), Nathan P. Gillett (Canada), Paul Ginoux (United States of America), Paul T. Griffiths (United Kingdom), Jian He (United States of America/China), Christopher Jones (United Kingdom), Svitlana Krakovska (Ukraine), Chaincy Kuo (United States of America), David S. Lee (United Kingdom), Maurice Levasseur (Canada), Martine Lizotte (Canada), Thomas K. Maycock (United States of America), Jean-François Müller (Belgium), Helène Muri (Norway), Lee T. Murray (United States of America), Zebedee R. J. Nicholls (Australia), Jurgita Ovadnevaite (Ireland/Lithuania), Prabir K. Patra (Japan/India), Fabien Paulot (United States of America/France, United States of America), Pallav Purohit (Austria/India), Johannes Quaas (Germany), Joeri Rogelj (United Kingdom /Belgium), Bjørn H. Samset (Norway), Chris Smith (United Kingdom), Izuru Takayabu (Japan), Marianne Tronstad Lund (Norway), Alexandra P. Tsimpidi (Germany/Greece), Steven Turnock United Kingdom), Rita Van Dingenen (Italy/Belgium), Hua Zhang (China), Alcide Zhao (United Kingdom/China)

Review Editors:

Yugo Kanaya (Japan), Michael J. Prather (United States of America), Noureddine Yassaa (Algeria)

Chapter Scientist:

Chaincy Kuo (United States of America)

This Supplementary Material should be cited as:

Naik, V., S. Szopa, B. Adhikary, P. Artaxo, T. Berntsen, W. D. Collins, S. Fuzzi, L. Gallardo, A. Kiendler Scharr, Z. Klimont, H. Liao, N. Unger, P. Zanis, 2021, Short-Lived Climate Forcers Supplementary Material. In: *Climate Change 2021: The Physical Science Basis. Contribution of Working Group I to the Sixth Assessment Report of the Intergovernmental Panel on Climate Change* [Masson-Delmotte, V., P. Zhai, A. Pirani, S. L. Connors, C. Péan, S. Berger, N. Caud, Y. Chen, L. Goldfarb, M. I. Gomis, M. Huang, K. Leitzell, E. Lonnoy, J. B. R. Matthews, T. K. Maycock, T. Waterfield, O. Yelekçi, R. Yu and B. Zhou (eds.)]. Available from <https://ipcc.ch/static/ar6/wg1>.

Date: August 2021

This document is subject to copy-editing, corrigenda and trickle backs.

Table of Contents

1	Table of Contents	
2		
3		
4	6.SM.1 Methodology for Emission based ERF.....	3
5	6.SM.2 ERF and GSAT timeseries from emulators for individual compounds over the historical period....	3
6	6.SM.3 Regression coefficient of annual mean surface ozone and PM _{2.5} against annual surface temperature	
7	change.....	5
8	6.SM.4 Effect on GSAT of a one year pulse of present-day emissions after 20 and 100 years.....	7
9	6.SM.5 Methodology to compute source sector apportionment for surface air pollutants using TM5-FASST	
10	8
11	6.SM.6 Data Table	11
12	References	26

ACCEPTED VERSION
SUBJECT TO FINAL EDITING

1 6.SM.1 Methodology for Emission based ERF

2 Emission-based ERFs are assessed (Figure 6.12) based on multi-model attribution experiments performed
3 under AerChemMIP (Collins et al., 2017) and analyzed by (Thornhill et al., 2021). The attribution
4 experiments are done with the precursors emissions individually perturbed (except CO and NMVOCs that
5 were done together). Due to the non-linear chemistry and microphysics of the atmosphere, the sum of the
6 emission-based contributions to ERF will not be equal to the concentration-based estimates (Figure 7.6)

7
8 The simulations in (Thornhill et al., 2021) are for the 1850-2014, and estimates for the emission-based ERFs
9 have been extrapolated to the full 1750-2019 period based on the updated emission estimates from the 11
10 September 2020 version of the Community Emissions Data System (CEDS) is used (Hoesly et al., 2018),
11 obtained from <https://doi.org/10.5281/zenodo.4025316> (cf 7.SM.1.4)

12
13 For the ozone ERF, in the AerChemMIP experiments the methane concentrations have been kept fixed when
14 the individual precursors are perturbed (e.g. NO_x). This means that methane is not governed by its emissions
15 and the atmospheric chemistry. Thus, adjustments have been done to consider the differences between CH₄
16 concentrations that would have been reached in a free to adjust simulation and a CH₄-fixed simulation. As a
17 consequence of this CH₄ adjustment, a correction has to be applied to all the chemical species which are
18 affected by CH₄ modification, either through chemistry itself (e.g. lifetime) or through stratospheric H₂O
19 changes and cloud changes. Despite these corrections, some non-linear effects in the chemistry can not be
20 fully captured and result in differences between the emission-based radiative forcing and the concentration-
21 based radiative forcing (Figure 7.6 and 7.SM.1.4). So finally, only the proportion of the individual effect is
22 kept from this methodology and applied to the concentration-based ERF which has been determined in a way
23 that allow to consider all the non-linearities.

24
25 The emission based ERF estimates for aerosols and aerosol precursors are based on the AerChemMIP
26 simulations (Thornhill et al., 2021). The contribution from aerosol radiation interaction (ari) is calculated as
27 the difference between the total ERF and ERFaci. Thus, the non-cloud adjustments are included as aerosol
28 radiation interaction. For NH₃ emissions ERFaci was not available, the ERF is contributed only to aerosol
29 radiation interaction. As for the ozone precursors, only the proportion of the individual effect is kept from
30 this methodology and applied to the concentration-based ERF .

31
32 For CO₂ the fraction of CO₂ in the atmosphere originating from anthropogenic emissions of non-CO₂
33 emissions must be subtracted from the concentration based estimate. The sum of Carbon emissions over the
34 historical period of CH₄, halocarbons, NMVOC + CO is estimated to be 6.6, 0.02, 26 Gt(C) respectively.
35 This includes a rough assumption that 25%, 0%, 50%, 0% (CH₄, halocarbons, NMVOC, CO) of reactive
36 intermediates such as formaldehyde are lost to deposition. Also assumes that 12% of methane C is still in the
37 atmosphere as methane (Stevenson et al., 2013). Using the (Joos et al., 2013) CO₂ response function to
38 convolve the time profile of emissions gives a rise in CO₂ of 110 ppb that is proportionally subtracted from
39 the CO₂ total.

40 For the halogenated species, the ERFs for CFCs and HCFCs are taken from Thornhill et al. (2021), and
41 adjusted to include emissions up to 2019. The ERF from HFCs, taken from the concentration-based
42 estimates (7.SM.1.4) are added, neglecting small effects through changes in OH concentrations affecting
43 HFC lifetime.

46 6.SM.2 ERF and GSAT timeseries from emulators for individual compounds over the historical period

47
48 GSAT change in response to ERF from SLCFs has been estimated using an emulator (see cross chapter box
49 7.1 and 7.SM.2) and presented in Figures 6.12, 6.15, 6.22 and 6.24. The emulator used is an impulse
50 response function (IRF) based on the two-layer energy balance model.

51 When the ERF time series is known, the response in GSAT at time *t* is given by:

$$52 GSAT(t) = \int_{t'=0}^t ERF(t') \cdot IRF(t - t') dt'$$

53 Where t'=0 denotes the time when the emission perturbation started, e.g. anthropogenic emissions since
54 1750.

1 The IRF used here has been calibrated according to the procedure given in 7.SM.2, and is given by:

2

3

$$IRF(t) = \sum_{j=1}^J \frac{c_j}{d_j} \exp\left(-\frac{t}{d_j}\right)$$

4 where the parameters c_j determine the equilibrium climate response and d_j are timescales of the fast and slow
5 modes of the climate system response, and $J=2$ here. The parameter values are: $d_1 = 3.4$ years and $d_2 = 285$
6 years, $c_1 = 0.44 \text{ K}/(\text{W m}^{-2})$ and $c_2 = 0.32 \text{ K}/(\text{W m}^{-2})$, corresponding to an ECS of 3.0K.

7 Figure 6.12 shows the historical emission based contributions to GSAT (1750-2019). For this analysis the
8 emission based ERF time series are based on the AerChemMIP simulations (Thornhill et al., 2021), and
9 described in 6.SM.1 and 7.SM.1.4. The emission-based assessment of ERF (6.SM.1) provides ERFs for 2019
10 relative to 1750, and to establish the ERF time series over the whole historical period, these were scaled back
11 according the historic emissions, i.e. assuming a liner relation between emissions and ERF historically.

12 Figure 6.15 shows the GSAT response to step emission reductions of idealized climate forcers with different
13 lifetimes. All forcers are assumed to give an ERF of -1.0 W m^{-2} when a new equilibrium concentration is
14 reached. With this assumption the ERF(t) is given by:

15 $ERF(t) = -1.0 \text{ W m}^{-2} \cdot (1 - e^{-\frac{t}{\tau}})$

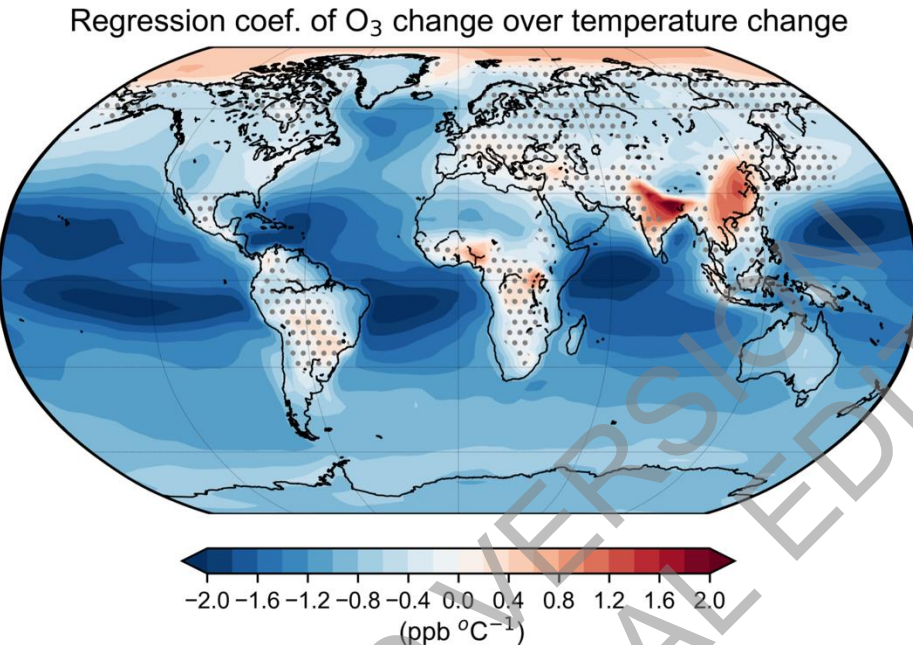
16 Where τ is the atmospheric lifetime of the climate forcer.

17 Figure 6.22 and 6.24 show the contributions to GSAT from individual SLCFs, or groups of SLCFs, with an
18 abundance-based perspective. The ERF time series are from the assessment of chapter 7 of this report and
19 details are given in 7.SM.1.4.

20

1
2 **6.SM.3 Regression coefficient of annual mean surface ozone and PM_{2.5} against annual surface**
3 **temperature change.**

4
5
6 [START FIGURE 6.SM.1 HERE]

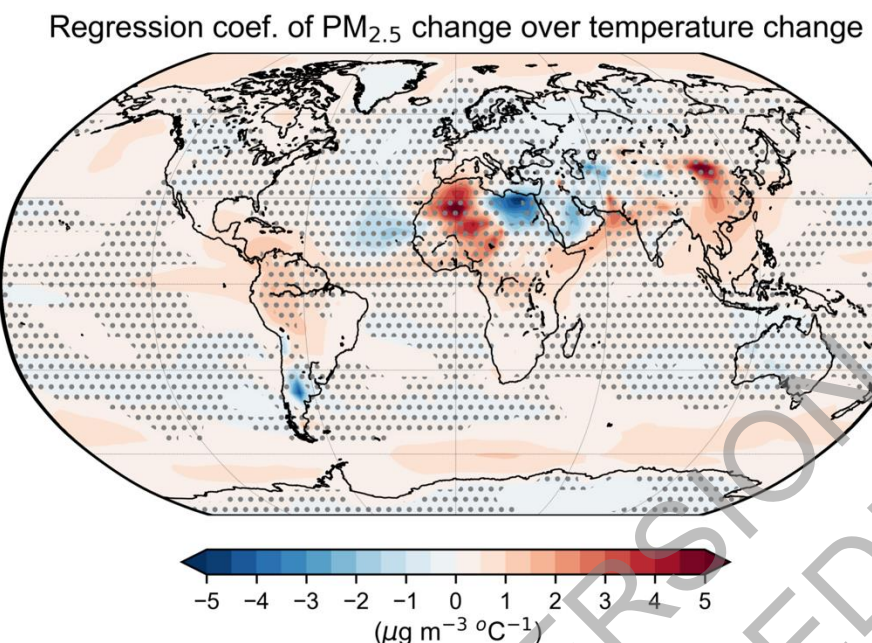


7
8 **Figure 6.SM.1:** Spatial pattern of the regression coefficient of annual surface ozone change (ssp370SST-
9 ssp370pdSST) over annual surface temperature change (ssp370SST-ssp370pdSST) (ppb °C⁻¹) during
10 the time period from 2015 to 2100, for the CMIP6 ensemble average (GFDL-ESM4, GISS-E2-1-G,
11 MRI-ESM2-0, UKESM1-0-LL). Regions without dots indicate that modelled regression coefficients
12 are statistically significant (at the 95% significance level) and agree on the sign for at least three out of
13 four models.
14

15 [END FIGURE 6.SM.1 HERE]
16
17
18
19
20
21
22
23
24
25
26
27
28
29
30
31
32
33
34
35

1 [START FIGURE 6.SM.2 HERE]

2



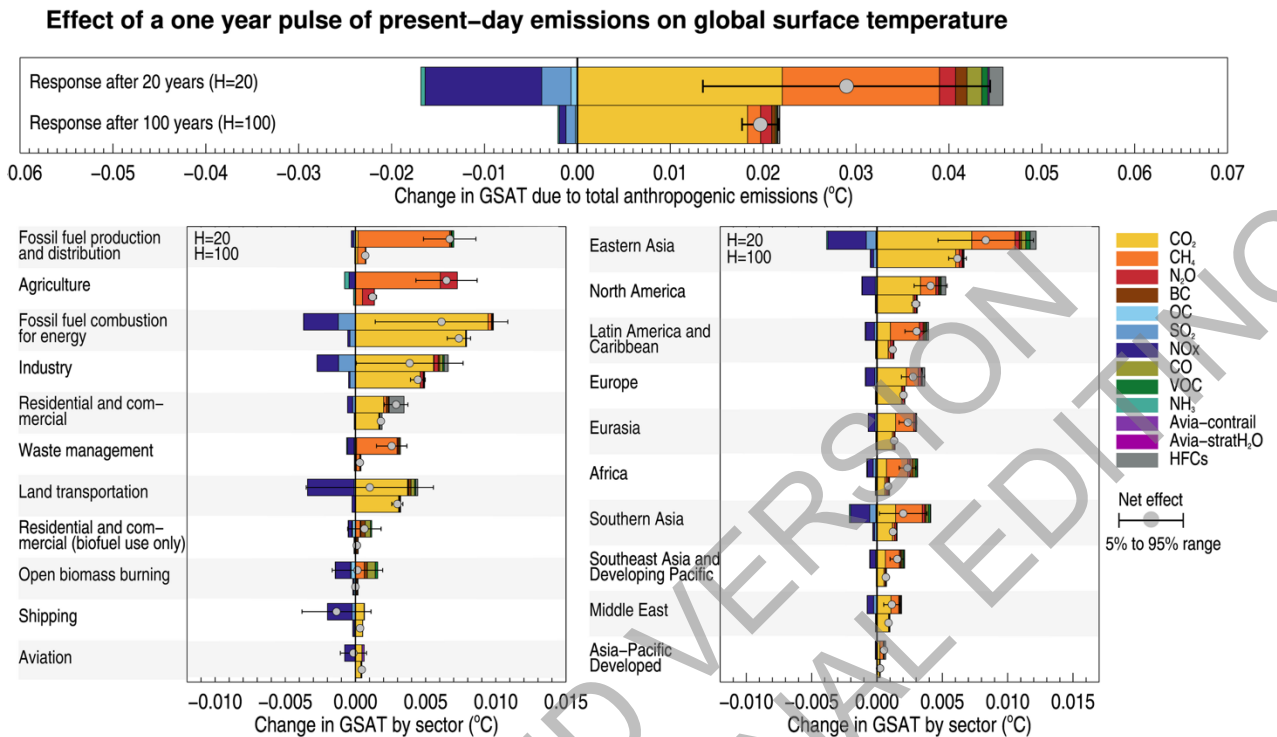
3
4 **Figure 6.SM.2:** Spatial pattern of the regression coefficient of annual surface PM_{2.5} concentrations change
5 (ssp370SST-ssp370pdSST) over annual surface temperature change (ssp370SST-ssp370pdSST) (μg
6 $\text{m}^{-3} \text{ }^{\circ}\text{C}^{-1}$) during the time period from 2015 to 2100, for the CMIP6 ensemble average (GFDL-ESM4,
7 GISS-E2-1-G, MRI-ESM2-0). Regions without dots indicate that modelled regression coefficients
8 are statistically significant (at the 95% significance level) and agree on the sign for at least two out of
9 three models.

10 [END FIGURE 6.SM.2 HERE]

11

12

13

1 **6.SM.4 Effect on GSAT of a one year pulse of present-day emissions after 20 and 100 years.**2
3
4
5
6**[START FIGURE 6.SM.3 HERE]**7 **Figure 6.SM.3:** Global-mean temperature response 20 and 100 years following one year of present-day (year 2014)
8 emissions.
910 **[END FIGURE 6.SM.3 HERE]**
1112
13
14 The temperature responses in Figure 6.16 and 6.SM.3 were calculated using the concept of absolute global
15 temperature change potential (AGTP) (Shine et al., 2005), i.e., an emission-metric-based emulator of the
16 climate response to individual emitted species. The approach and further details are documented in Lund et
17 al. (2020). The emissions were taken from the Community Emissions Data System (CEDS) for year 2014
18 (Hoesly et al., 2018), with the exceptions of HFCs, which originate from Purohit et al. (2020) and consider
19 HFCs with a lifetime shorter than 50 years, open biomass burning from van Marle et al. (2017), and aviation
20 water vapour from Lee et al. (2020). The split between fossil fuel and biofuel emissions in the residential
21 sector, and between the fossil fuel production and distribution and combustion in the energy sector, is based
22 on the GAINS model (ECLIPSE version 6b dataset:
23 https://iiasa.ac.at/web/home/research/researchPrograms/air/Global_emissions.html). CO₂ emissions are
24 excluded from open biomass burning and residential biofuel use due to their unavailability in CEDS and
25 uncertainties around non-sustainable emission fraction.26 Aviation specific AGTPs have been calculated for Figure 6.SM.3 using the method described in Lund et al.
27 (2020) and the best estimate radiative forcing values from Lee et al. (2020). For the HFCs, the AGTPs were
28 derived from Hodnebrog et al. (2020). The AGTPs of BC, SO₂ and OC account for the direct aerosol effect
29 due to aerosol-radiation interactions and are scaled to account for the semi-direct of BC due to rapid
30 adjustments and indirect radiative forcing through aerosol-cloud interactions of sulfate aerosols, respectively.
31 All AGTPs used in the temperature response calculations now include a carbon-climate feedback term based
32 on the framework by Gasser et al. (2017), except those for HFCs. Avia-contrail refers to the impact from
33 linear contrail formation and subsequent spreading to cirrus clouds and Avia-stratH₂O to the direct impact of
34 aircraft water vapour emissions.
35

- 1 The error bars show the range (5-95% interval) in net temperature impact due to uncertainty in radiative
 2 forcing *only*. This uncertainty range is calculated using a Monte Carlo approach and estimates of
 3 uncertainties in global-mean RF of individual species from the literature - see Lund et al. (2020) for details.
 4 The uncertainty in the RF of individual halocarbons was not included due to lack of available data.
 5
 6 The AGTP applies an impulse response function (IRF) to calculate the temperature response as a function of
 7 time to a given forcing. The IRF is given by:

$$8 \quad IRF(t) = \sum_{j=1}^J \frac{c_j}{d_j} \exp\left(-\frac{t}{d_j}\right)$$

9
 10 where c_j and d_j are constants and timescales of the fast and slow model of the climate system response,
 11 respectively, and $j=2$ here. The IRF used in Lund et al. (2020) is based on Geoffroy et al. (2013), which
 12 yields $d_1 = 4.1$ years and $d_2 = 249$ years, $c_1 = 0.519 \text{ K}/(\text{Wm}^{-2})$ and $c_2 = 0.365 \text{ K}/(\text{Wm}^{-2})$, corresponding to an
 13 ECS of 3.5K. Note that the IRF used for calculations of GSAT for figures 6.12, 6.15, 6.22 and 6.24 use an
 14 IRF calibrated to the assessment of ECS and TCR as given in Chapter 7 of this report, and thus use slightly
 15 different values for the c_j and d_j constants (see 6.SM.2).

16
 17
 18 **6.SM.5 Methodology to compute source sector apportionment for surface air pollutants using TM5-**
 19 **FASST**

20 Here we provide description of the methodology used to calculate the source sector apportionment for PM_{2.5}
 21 and ozone (Figure 6.17). Furthermore, Figures 6.SM4 and 6.SM.5 show a comparison of TM5-FASST and
 22 ESM models responses to changes in emissions of PM_{2.5} precursors and ozone.

23 TM5-FASST is a reduced-form source-receptor model, describing the surface level spatial response of a
 24 pollutant metric (concentration, exposure, deposition) to changes in precursor emissions. The model is
 25 constructed from pre-computed emission-concentration transfer matrices between pollutant source regions
 26 and receptor regions. These matrices reflect underlying meteorological and chemical atmospheric processes
 27 for a predefined set of meteorological and emission data and have the advantage that concentration responses
 28 to emission changes are obtained by a simple matrix multiplication, avoiding expensive numerical
 29 computations.

30 TM5-FASST's source-receptor matrices have been derived with the chemistry-transport model TM5, by
 31 applying 20% emission perturbations on a reference emission set (RCP year 2000, year 2001 meteorology)
 32 for individual precursors and 56 source regions. The total concentration of component (or metric) j in
 33 receptor region y , resulting from given emissions E of all n_i precursors i at all n_x source regions x , is obtained
 34 as a perturbation on the base-simulation concentration, by summing up all the respective source-receptor
 35 coefficients A , scaled with the actual emission perturbation:

$$36 \quad C_j(y) = C_{j,\text{ref}}(y) + \sum_{k=1}^{n_x} \sum_{i=1}^{n_i} A_{ij}[x_k, y] \cdot [E_i(x_k) - E_{i,\text{ref}}(x_k)] \quad (1)$$

37 where $A_{ij}[x_k, y] = \frac{\Delta C_{j,\text{ref}}(y)}{0.2E_{i,\text{ref}}(x_k)}$, the pre-computed source-receptor coefficient for source region x_k to receptor
 38 region y , for precursor i contributing to metric/pollutant j . The computational efficiency from the linearized
 39 emission-concentration sensitivities comes at some cost of accuracy, in particular because the model
 40 bypasses underlying mechanisms describing chemical and meteorological feedback processes that could lead
 41 to non-linear responses.

42 TM5-FASST computes PM_{2.5} concentrations from precursor emissions of SO₂, NO_x, NH₃, elemental carbon
 43 and particulate organic matter. Secondary organic matter from anthropogenic emissions is not included.
 44 Ozone concentrations and long-term exposure metrics are computed from NO_x, non-methane volatile organic
 45 compounds (NMVOC) and methane precursor emissions. CO as ozone precursor is not included. The
 46 methane-ozone response is assumed to be instantaneous, neglecting the 11 year response time (Fiore et al.,

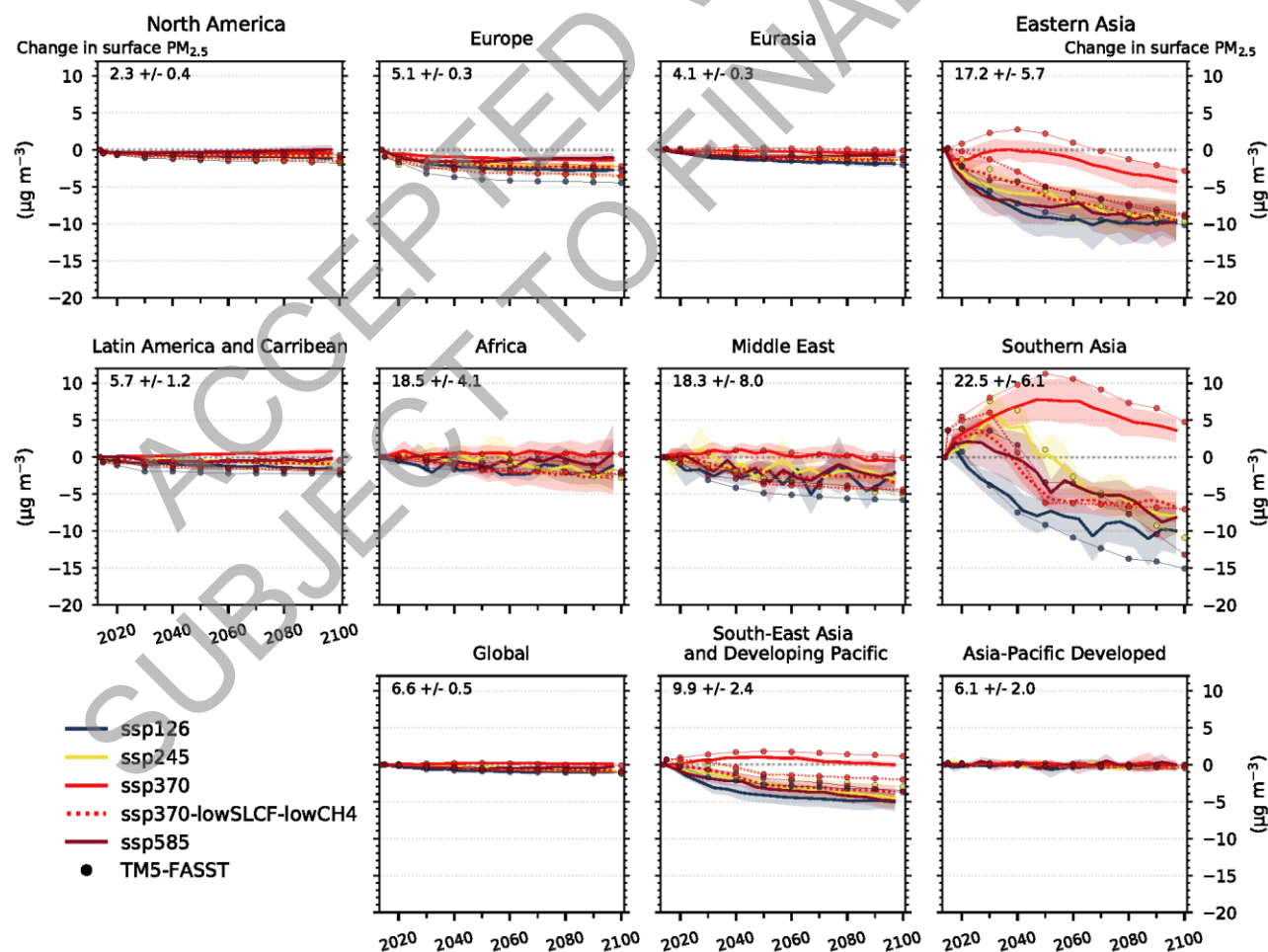
1 2008)

2
3 The computational efficiency of TM5-FASST allows for multiple runs exploring source attribution by region
4 or emission source. We estimate the relative contribution of individual emission sectors shown in Figure
5 6.17 by subtracting their emissions one by one from the total emissions in Eq. (1) and computing the
6 resulting concentration. Subtracting this result from the total concentration (Eq. 1) yields each sector's
7 contribution (Karagulian et al., 2016).

8
9 TM5-FASST has been extensively documented and evaluated by (Van Dingenen et al., 2018). The model
10 has been applied in a variety of assessment studies (e.g., Aakre et al., 2018; Brauer et al., 2016; Crippa et al.,
11 2019; Harmsen et al., 2020; Kühn et al., 2020; Markandya et al., 2018; Rao et al., 2017; Raut et al., 2020;
12 Vandyck et al., 2020). Validation studies in Van Dingenen et al. (2018) show that, despite inherent
13 simplifications and caveats, large scale PM_{2.5} and O₃ responses to emission changes in TM5-FASST
14 compare well with the chemical transport model TM5. Figure 6.SM.4 and 6.SM.5 compare TM5-FASST
15 regional PM_{2.5} and O₃ responses to emission changes with the ensemble of ESM models for selected SSP
16 scenarios. In nearly all cases TM5-FASST results fall within ± 1 standard deviation of the CMIP6 ESM
17 ensemble. Notable differences are observed for the SSP scenarios and regions representing more extreme
18 emission changes (in particular for the low emission scenarios in Southern Asia). As documented by Van
19 Dingenen et al. (2018), both for PM_{2.5} and O₃ the differences with full process models can be attributed to
20 non-linear responses to NO_x emission reductions that are not captured by the linearized source-receptor
21 model.

22
23 [START FIGURE 6.SM.4 HERE]

24
25
26



27

Figure 6.SM.4: Future global and regional changes in annual mean surface PM_{2.5}, relative to 2005-2014 mean, for the different SSPs used in CMIP6. Each line represents a multi-model mean across the region with shading representing the ± 1 standard deviation in the mean. Dots represent TM5-FASST results. The multi-model regional mean value (± 1 standard deviation) for the year 2005-2014 is shown in the top left corner of each panel.

[END FIGURE 6.SM.4 HERE]

[START FIGURE 6.SM.5 HERE]

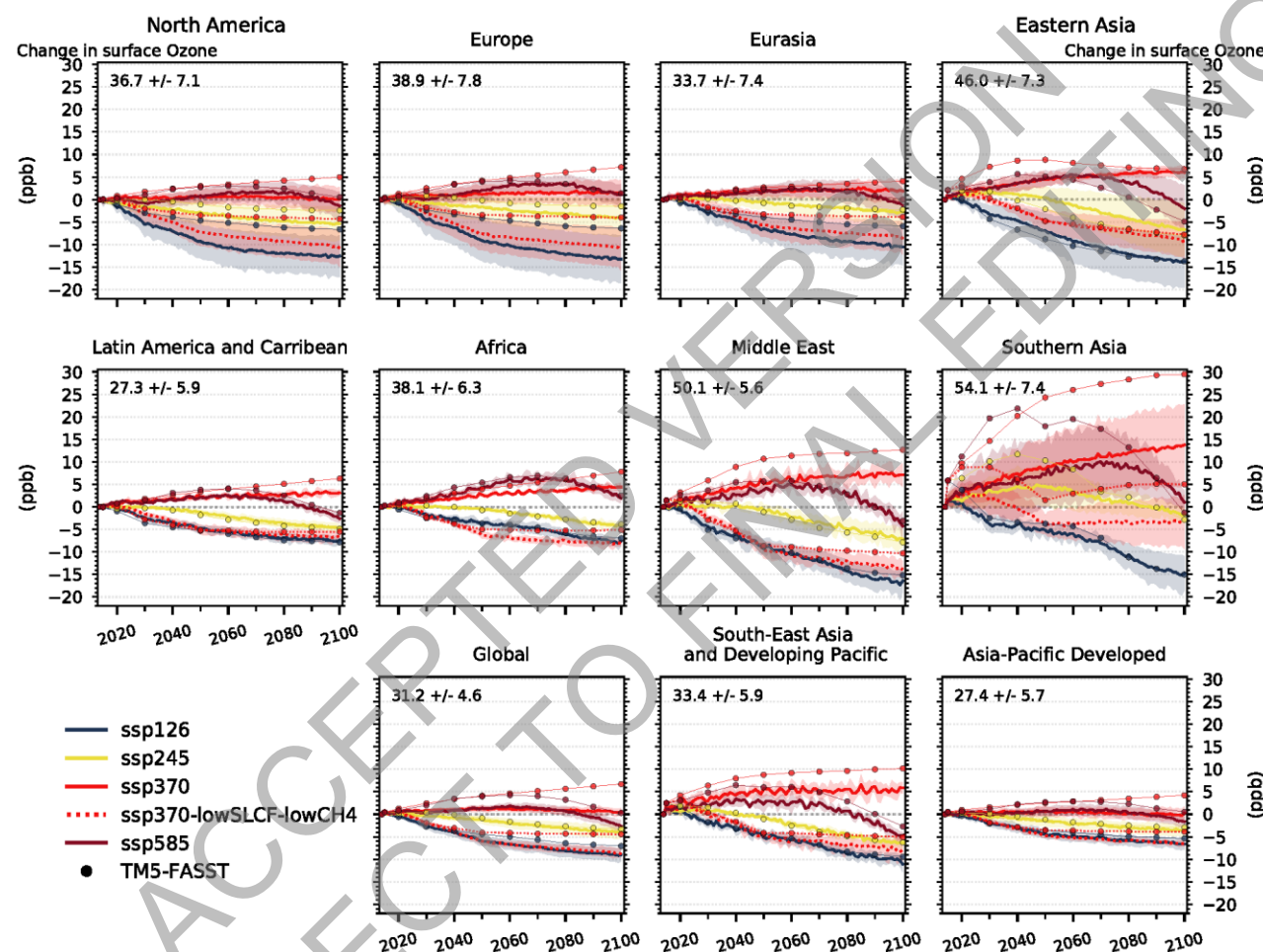


Figure 6.SM.5: Future global and regional changes in annual mean surface O₃, relative to 2005-2014 mean, for the different SSPs used in CMIP6. Each line represents a multi-model mean across the region with shading representing the \pm standard deviation in the mean. Dots represent TM5-FASST results. The multi-model regional mean value (± 1 standard deviation) for the year 2005-2014 is shown in the top left corner of each panel.

[END FIGURE 6.SM.5 HERE]

1 **6.SM.6 Data Table**

2

3

4 **[START TABLE 6.SM.1 HERE]**

5

6 **Table 6.SM.1:** Input Data Table. Input datasets and code used to create chapter figures.

7

8

Figure number/Table number/Chapter section (for calculations)	Dataset name	Type of dataset	Filename	License type	Dataset citation	Dataset DOI/URL	Citation for relevant papers
Figure 6.3	Community Emissions Data System (CEDS)	Input dataset		Public	(Hoesly et al., 2018)	http://www.globalchange.umd.edu/ceds/	
Figure 6.4	CMIP6, ScenarioMIP, Tropospheric Ozone Assessment Report (TOAR), Atmospheric Chemistry and Climate Model Intercomparison Project (ACCMIP)	Input dataset	CMIP6 Models UKESM1-LL-0, CESM2-WACCM, GFDL-ESM4, MRI-ESM2-0, GISS-E2.1-G. Experiments : Historical experiment, ssp370	public	(Eyring et al., 2016; O'Neill et al., 2016)	https://esgf-node.llnl.gov/search/cmip6/	(Young et al., 2013, 2018; DuplicateGriffiths et al., 2020)
	Observational datasets TOST, IASI-FORLI, IASI-OFRID, OMI/MLS, OMI-SAI, OMI-RAL:	Input dataset		public		https://doi.org/10.1525/elementa.291.t1	(Gaudel et al., 2018)

CMIP6 model data							
CESM2-WACCM: historical, ssp370	Input dataset			(Danabas oglu, 2019b, 2019c)			
GFDL-ESM4: esm-hist, historical, ssp370	Input dataset			(John et al., 2018c; Krasting et al., 2018b, 2018a)			
GISS-E2-1-G: historical, ssp370	Input dataset			(NASA Goddard Institute for Space Studies (NASA/G ISS), 2018, 2020h)			
MRI-ESM2-0: historical, ssp370	Input dataset			(Yukimot o et al., 2019g, 2019c)			
UKESM1-0-LL: historical, ssp370	Input dataset			(Good et al., 2019c; Tang et al., 2019)			
Figure 6.5	IAGOS-CORE	Input dataset	decadal	public	(Gaudel et al., 2020)	http://www.iagos-data.fr/portal.html#TimeseriesPlace:	(Cooper et al., 2020)
Figure 6.6	Merged GOME/SCIAMAC HY/GOME-2 (TM4NO2A)	Input dataset	GOME_SCIAMACHY_GOME2a b_TroposNO2_v2.3_041996- 092017_temis.nc	public		http://www.temis.nl/airpollution/no2.htm	(Georgoulias et al., 2019)

	version 2.3)						
Figure 6.7	EPA PM _{2.5} aerosol component	Input dataset	Monthly-average 2000-2018	public		https://aqs.epa.gov/aqsweb/airdata/downloa_d_files.html	(Solomon et al., 2014)
	IMPROVE aerosol	Input dataset	Monthly-average daily 2000-2018	public		http://views.cira.colostate.edu/fed/QueryWizard/Default.aspx	
	EMEP PM _{2.5} aerosol component	Input dataset	Monthly-average 2000-2018	public		https://www.emep.int/	
	Network Center for EANET, EANET Data on the Acid Deposition in the East Asian Region, PM _{2.5} aerosol component	Input dataset	Monthly-average 2001-2017	public		https://www.eanet.asia/document/public/index	
	SPARTAN PM _{2.5} aerosol component	Input dataset	Monthly-average 2013-2019	public		https://www.spartan-network.org/	(Snider et al., 2015)
	observational field campaigns PM _{2.5} aerosol component over Latin America and Caribbean, Africa, Europe, Eastern Asia, and Asia-Pacific Developed	Input dataset		public			(Celis et al., 2004; Feng et al., 2006; Mariani and de Mello, 2007; Molina et al., 2007, 2010; Bourotte et al., 2007; Fuzzi et al., 2007; Mkoma, 2008; Favez et al., 2008; Aggarwal and Kawamura, 2009; Mkoma et al., 2009; Li et al., 2010; Martin et al., 2010; Radhi et al., 2010; Weinstein et

							al., 2010; de Souza et al., 2010; Batmunkh et al., 2011; Pathak et al., 2011; Gioda et al., 2011; Zhang et al., 2012; Zhao et al., 2013; Cho and Park, 2013; Wang et al., 2019; Kuzu et al., 2020)
		Intermediate dataset				Code to be placed in https://github.com/IPCC-WG1	
Figure 6.8	CMIP6 Ambient Aerosol Optical Thickness at 550nm	Input dataset Annual average	historical experiment, Models ACCESS-CM2, BCC-ESM1, CESM2-FV2,CESM2-WACCM,CESM2,CNRM-CM6-1,CNRM-EMS2-1,CanESM5,E3SM-1-0,GFDL-CM4,GFDL-ESM4,GISS-E2-1-G,HadGEM3-GC31-LL,INM-CM4-8,IPSL-CM6A-LR,KACE-1-0-G,MIROC-ES2L,MPI-ESM-1-2,MPI-ESM1-2-HR,MPI-ESM1-2-LR,MRI-ESM2-0,NorESM2-LM,UKESM1-0-LL	(Eyring et al., 2016; O'Neill et al., 2016)			
Figure 6.9	CMIP6, mole fraction hydroxyl in air	Input dataset Decadal average	Models UKESM1-0LL, GFDL-ESM4, CESM2-WACCM	public	(Eyring et al., 2016)	https://esgf-node.llnl.gov/search/cmip6/	(Montzka et al., 2011; Rigby et al., 2017; Turner et al., 2017;

						Nicely et al., 2018; Naus et al., 2019; Patra et al., 2021)
CMIP6 model data						
CESM2-WACCM: historical	Input dataset			(Danabaso glu, 2019b)		
GFDL-ESM4: historical	Input dataset			(Krasting et al., 2018b)		
UKESM1-0-LL: historical	Input dataset			(Tang et al., 2019)		
Figure 6.10	CMIP6: AerChemMIP experiments histSST and histSST-piAer. Output variable rsut and rlut	Input dataset Average d from monthly output Intermediate dataset	Models, MIROC6, MPI-I-ESM-1-2-HAM, GISS-E2-1-G, NorESM2-LM, MRI-ESM2-0, GFDL-ESM4, UKESM-0-LL	public (Eyring et al., 2016; Collins et al., 2017)	https://esgf-node.llnl.gov/search/cmip6/ Code to be placed in https://github.com/IPCC-WG1 TBD	(Myhre et al., 2013)
CMIP6 model data						
GFDL-ESM4: histSST, histSST-piAer	Input dataset			(Horowitz et al., 2018b, 2018a)		
GISS-E2-1-G: histSST, histSST-piAer	Input dataset			(NASA Goddard Institute for Space Studies (NASA/GI SS), 2019a, 2019b)		

	MIROC6: histSST, histSST-piAer	Input dataset			(Takemura , 2019a, 2019b)		
	MPI-ESM-1-2-HAM: histSST, histSST-piAer	Input dataset			(Neubauer et al., 2019b, 2019a)		
	MRI-ESM2-0: histSST, histSST-piAer	Input dataset			(Yukimoto et al., 2019a, 2020a)		
	NorESM2-LM: histSST, histSST-piAer	Input dataset			(Olivière et al., 2019b, 2019a)		
	UKESM1-0-LL: histSST, histSST-piAer	Input dataset			(O'Connor , 2019b, 2019a)		
Figure 6.11	CMIP6: AerChemMIP experiments histSST and histSST-piAer. Output variable rsut and rlut	Input dataset Average d from monthly output	Models, MIROC6, MPI-I-ESM-1-2-HAM, GISS-E2-1-G, NorESM2-LM, MRI-ESM2-0, GFDL-ESM4, UKESM-0-LL	public	(Eyring et al., 2016; Collins et al., 2017)	https://esgf-node.llnl.gov/search/cmip6/ Code to be placed in https://github.com/IPCC-WG1 TBD	(Myhre et al., 2013)
Data citations							
	GFDL-ESM4: histSST, histSST-piAer	Input dataset			(Horowitz et al., 2018b, 2018a)		
	GISS-E2-1-G: histSST, histSST-piAer	Input dataset			(NASA Goddard Institute for Space Studies (NASA/GI SS), 2019a,		

				2019b)		
MIROC6: histSST, histSST-piAer	Input dataset			(Takemura , 2019a, 2019b)		
MPI-ESM-1-2-HAM: histSST, histSST-piAer	Input dataset			(Neubauer et al., 2019b, 2019a)		
MRI-ESM2-0: histSST, histSST-piAer	Input dataset			(Yukimoto et al., 2019a, 2020a)		
NorESM2-LM: histSST, histSST-piAer	Input dataset			(Olivière et al., 2019b, 2019a)		
UKESM1-0-LL: histSST, histSST-piAer	Input dataset			(O'Connor , 2019b, 2019a)		
Figure 6.12	CMIP6,	Input dataset		(Eyring et al., 2016)	https://esgf-node.llnl.gov/search/cmip6/ Code to be placed in https://github.com/IPCC-WG1 TBD	(Ghan, 2013; Duplicate Thornhill et al., 2021)
Figure 6.13	CMIP6: AerChemMIP experiments historical and hist-piAer. Output variable tas	Intermediate dataset	Models MIROC6, MRI-ESM2-0, NorESM2-LM, GFDL-ESM4, GISS-E2-1-G, UKESM1-0-LL.	(Eyring et al., 2016; Collins et al., 2017)	Code to be placed in https://github.com/IPCC-WG1 TBD	
Figure 6.14	CMIP6 historical experiment, AerChemMIP experiments ssp370 ssp370SST, ssp370pdSST experiments.	Input dataset Monthly mean	Models GFDL-ESM4, GISS-E2-1-G, MRI-ESM2-0, UKESM1-0-LL	public	(Eyring et al., 2016; Collins et al., 2017) https://esgf-node.llnl.gov/search/cmip6/ Code to be placed in https://github.com/IPCC-WG1 TBD	

	Output variables o3, tas						
Data citations							
	GFDL-ESM4: ssp370SST, ssp370pdSST	Input dataset		(Horowitz et al., 2018c, 2018d)			
	GISS-E2-1-G: ssp370SST, ssp370pdSST	Input dataset		(NASA Goddard Institute for Space Studies (NASA/GI SS), 2020b, 2020a)			
	MRI-ESM2-0: ssp370SST, ssp370pdSST	Input dataset		(Yukimoto et al., 2019b, 2020b)			
	UKESM1-0-LL: ssp370pdSST, ssp370SST	Input dataset		(O'Connor 2020b, 2020a)			
Figure 6.15	CMIP6, ScenarioMIP experiments ssp370SST, ssp370pdSST Mole fraction of ozone	Input dataset OUTPU T DATA FREQU ENCY	Models GFDL-ESM4, GISS-E2-1-G, MRI-ESM2-0, UKESM1-0-LL	public	(Eyring et al., 2016; O'Neill et al., 2016)	https://esgf-node.llnl.gov/search/cmip6/	
Figure 6.16	CMIP6, ScenarioMIP experiments ssp370SST, ssp370pdSST	Input dataset OUTPU T DATA FREQU ENCY	CMIP6 models GFDL-ESM4, GISS-E2-1-G, MRI-ESM2-0 and UKESM1-0-LL	public	(Eyring et al., 2016; O'Neill et al., 2016)	https://esgf-node.llnl.gov/search/cmip6/	

Figure 6.17	CMIP6, ScenarioMIP Mole fraction of ozone	Input dataset Intermedia te data	GFDL-ESM4, BCC-ESM1, CESM2-WACCM and UKESM1- 0-LL for ssp370, GFDL-ESM4, BCC-ESM1, and CESM2- WACCM for ssp370-lowNTCF, GFDL-ESM4 and UKESM1-0-LL for SSP1-2.6, SSP2-4.5 and SSP5- 8.5	public	(Eyring et al., 2016; O'Neill et al., 2016)	https://esgf-node.llnl.gov/search/cmip6/	
Figure 6.20 Figure 6.21	GEIA/ACCENT gridded emissions	Input dataset		public		http:// geiacenter.org	(Lamarque et al., 2010)
	Community Emissions Data System (CEDS) for Historical Emissions	Input dataset		public	(van Marle et al., 2017; Hoesly et al., 2018)	http://www.globalchange.umd.edu/ceds/ http://esgf-node.llnl.gov/search/input4mips/	
	SSP Database (Shared Socioeconomic Pathways) - Version 2.0,	Input dataset		public	(Riahi et al., 2017; Rogelj et al., 2018; Gidden et al., 2019)	https://tntcat.iiasa.ac.at/SspDb/dsd	
	Representative Concentration Pathway (RCP) database	Input dataset		public	(van Vuuren et al., 2011)	https://tntcat.iiasa.ac.at/RcpDb/dsd	
		Intermedia te dataset				https://github.com/gidden/ar6-wg1-ch6-emissions Code to be placed in https://github.com/IPCC-WG1	
CMIP6 model data in Figure 6.20							
	BCC-ESM1: ssp370, ssp370- lowNTCF, historical	Input dataset			(Zhang et al., 2018, 2019b, 2019a)		
	CESM2-WACCM: ssp370-lowNTCF, historical, ssp370	Input dataset			(Danabaso glu, 2019a, 2019b,		

				2019c)		
GFDL-ESM4: ssp370-lowNTCF, historical, ssp126, ssp245, ssp370, ssp585	Input dataset			(Horowitz et al., 2018a; John et al., 2018c, 2018d, 2018a, 2018b; Krasting et al., 2018b)		
GISS-E2-1-G: historical, ssp126, ssp245, ssp370, ssp370-lowNTCF, ssp585	Input dataset			(NASA Goddard Institute for Space Studies (NASA/GI SS), 2018, 2020i, 2020g, 2020e, 2020f, 2020h)		
MRI-ESM2-0: historical, ssp126, ssp245, ssp370, ssp370-lowNTCF, ssp585	Input dataset			(Yukimoto et al., 2019d, 2019h, 2019f, 2019e, 2019g, 2019c)		
UKESM1-0-LL: ssp370-lowNTCF, historical, ssp126, ssp245, ssp370, ssp585	Input dataset			(Good et al., 2019a, 2019d, 2019c, 2019b; Tang et al., 2019; Byun,		

				2020)		
CMIP6 model data in Figure 6.21						
BCC-ESM1: ssp370, ssp370- lowNTCF, historical	Input dataset			(Zhang et al., 2018, 2019b, 2019a)		
CESM2-WACCM: ssp370-lowNTCF, historical, ssp370	Input dataset			(Danabaso glu, 2019a, 2019b, 2019c)		
CNRM-ESM2-1: ssp370-lowNTCF, historical, ssp370	Input dataset			(Seferian, 2018, 2019; Volodire, 2019)		
GFDL-ESM4: ssp370-lowNTCF, historical, ssp126, ssp245, ssp370, ssp585	Input dataset			(Horowitz et al., 2018a; John et al., 2018c, 2018d, 2018a, 2018b; Krasting et al., 2018b)		
GISS-E2-1-G: ssp370-lowNTCF, historical, ssp126, ssp245, ssp370, ssp585	Input dataset			(NASA Goddard Institute for Space Studies (NASA/GI SS), 2018, 2020i, 2020g, 2020f, 2020a, 2020h)		
HadGEM3-GC31-	Input			(Good,		

	LL: historical, ssp126, ssp245, ssp585	dataset			2019, 2020b, 2020a; Ridley et al., 2019)		
	MIROC-ES2L: historical, ssp126, ssp245, ssp370, ssp585	Input dataset			(Hajima et al., 2019; Tachiiri et al., 2019a, 2019b, 2019d, 2019c)		
	MPI-ESM-1-2- HAM: ssp370- lowNTCF, historical, ssp370	Input dataset			(Neubauer et al., 2019b, 2019a)		
	MRI-ESM2-0: ssp370-lowNTCF, historical, ssp126, ssp245, ssp370, ssp585	Input dataset			(Yukimoto et al., 2019h, 2019f, 2019e, 2019g, 2019c, 2019a)		
Figure 6.22	NorESM2-LM: ssp370-lowNTCF, historical, ssp126, ssp245, ssp370, ssp585	Input dataset			(Olivière et al., 2019; Selander et al., 2019e, 2019d, 2019c, 2019b, 2019a)	https://esgf-node.llnl.gov/search/cmip6/	
Figure 6.23	UKESM1-0-LL: ssp370-lowNTCF, historical, ssp126, ssp245, ssp370, ssp585	Input dataset			(Good et al., 2019a, 2019d, 2019c, 2019b; Tang et al., 2019;	https://esgf-node.llnl.gov/search/cmip6/	

Figure 6.24	CMIP6, AerChemMIP Output variable rsut and rlut, monthly output ssp370SST and ssp370SST- lowNTCF	Input dataset	BCC-ESM1, CNRM-ESM2-1, CESM2-WACCM, and GFDL- ESM4.	public	(Byun, 2020) (Eyring et al., 2016; Collins et al., 2017)	https://esgf-node.llnl.gov/search/cmip6/	
Figure 6.25	ScenarioMIP, RCMIP Emulator output	Input dataset		public	(Eyring et al., 2016; O'Neill et al., 2016; Nicholls et al., 2020)	https://esgf-node.llnl.gov/search/cmip6/	(Geoffroy et al., 2013)
Figure 6.26	ScenarioMIP Emulator output	Input dataset		public	(O'Neill et al., 2016)	https://esgf-node.llnl.gov/search/cmip6/	(DuplicateLun d et al., 2020)
Figure 6.27	ScenarioMIP Emulator output	Input dataset		public	(O'Neill et al., 2016)	https://esgf-node.llnl.gov/search/cmip6/	
Figure 6.25 FGD						https://tntcat.iiasa.ac.at/SspDb/dsd	
Figure	CMIP6 model data						

6.SM.1	GFDL-ESM4: ssp370SST, ssp370pdSST	Input dataset		(Horowitz et al., 2018c, 2018d)		
	GISS-E2-1-G: ssp370SST, ssp370pdSST	Input dataset		(NASA Goddard Institute for Space Studies (NASA/GI SS), 2020d, 2020c)		
	MRI-ESM2-0: ssp370SST, ssp370pdSST	Input dataset		(Yukimoto et al., 2019b, 2020b)		
	UKESM1-0-LL: ssp370pdSST, ssp370SST	Input dataset		(O'Connor , 2020c, 2020b)		
Figure 6.SM.2	CMIP6 model data					
	GFDL-ESM4: ssp370SST, ssp370pdSST	Input dataset		(Horowitz et al., 2018c, 2018d)		
	GISS-E2-1-G: ssp370SST, ssp370pdSST	Input dataset		(NASA Goddard Institute for Space Studies (NASA/GI SS), 2020d, 2020c)		
	MRI-ESM2-0: ssp370SST, ssp370pdSST	Input dataset		(Yukimoto et al., 2019b, 2020b)		

	UKESM1-0-LL: ssp370pdSST, ssp370SST	Input dataset		(O'Connor , 2020c, 2020b)		
Figure 6.SM.4	CMIP6 model data					
	GFDL-ESM4: ssp370- lowNTCFCH4	Input dataset		(Horowitz et al., 2018b)		
	GISS-E2-1-G: ssp370- lowNTCFCH4	Input dataset		(NASA Goddard Institute for Space Studies (NASA/GI SS), 2020b)		
	MRI-ESM2-0: ssp370- lowNTCFCH4	Input dataset		(Yukimoto et al., 2020a)		
	UKESM1-0-LL: ssp370- lowNTCFCH4	Input dataset		(O'Connor , 2020a)		

1

2 [END TABLE 6.SM.6 HERE]

3

4

5

6

7

1 References

- Aakre, S., Kallbekken, S., Van Dingenen, R., and Victor, D. G. (2018). Incentives for small clubs of Arctic countries to limit black carbon and methane emissions. *Nat. Clim. Chang.* doi:10.1038/s41558-017-0030-8.
- Brauer, M., Freedman, G., Frostad, J., van Donkelaar, A., Martin, R. V., Dentener, F., et al. (2016). Ambient Air Pollution Exposure Estimation for the Global Burden of Disease 2013. *Environ. Sci. Technol.* 50, 79–88. doi:10.1021/acs.est.5b03709.
- Collins, W. J., Lamarque, J. F., Schulz, M., Boucher, O., Eyring, V., Hegglin, I. M., et al. (2017). AerChemMIP: Quantifying the effects of chemistry and aerosols in CMIP6. *Geosci. Model Dev.* 10, 585–607. doi:10.5194/gmd-10-585-2017.
- Crippa, M., Janssens-Maenhout, G., Guizzardi, D., Van Dingenen, R., and Dentener, F. (2019). Contribution and uncertainty of sectorial and regional emissions to regional and global PM_{2.5} health impacts. *Atmos. Chem. Phys.* 19, 5165–5186. doi:10.5194/acp-19-5165-2019.
- Fiore, A. M., West, J. J., Horowitz, L. W., Naik, V., and Schwarzkopf, M. D. (2008). Characterizing the tropospheric ozone response to methane emission controls and the benefits to climate and air quality. *J. Geophys. Res. Atmos.* doi:10.1029/2007JD009162.
- Fuglestvedt, J. S., Shine, K. P., Berntsen, T., Cook, J., Lee, D. S., Stenke, A., et al. (2010). Transport impacts on atmosphere and climate: Metrics. *Atmos. Environ.* 44, 4648–4677. doi:10.1016/j.atmosenv.2009.04.044.
- Gasser, T., Peters, G. P., Fuglestvedt, J. S., Collins, W. J., Shindell, D. T., and Ciais, P. (2017). Accounting for the climate–carbon feedback in emission metrics. *Earth Syst. Dyn.* 8, 235–253. doi:10.5194/esd-8-235-2017.
- Geoffroy, O., Saint-Martin, D., Olivié, D. J. L., Volodire, A., Bellon, G., and Tytéca, S. (2013). Transient Climate Response in a Two-Layer Energy-Balance Model. Part I: Analytical Solution and Parameter Calibration Using CMIP5 AOGCM Experiments. *J. Clim.* 26, 1841–1857. doi:10.1175/JCLI-D-12-00195.1.
- Harmsen, M. J. H. M., van Dorst, P., van Vuuren, D. P., van den Berg, M., Van Dingenen, R., and Klimont, Z. (2020). Co-benefits of black carbon mitigation for climate and air quality. *Clim. Change.* doi:10.1007/s10584-020-02800-8.
- Hodnebrog, Ø., Aamaas, B., Fuglestvedt, J. S., Marston, G., Myhre, G., Nielsen, C. J., et al. (2020). Updated Global Warming Potentials and Radiative Efficiencies of Halocarbons and Other Weak Atmospheric Absorbers. *Rev. Geophys.* 58, e2019RG000691. doi:<https://doi.org/10.1029/2019RG000691>.
- Hoesly, R. M., Smith, S. J., Feng, L., Klimont, Z., Janssens-Maenhout, G., Pitkanen, T., et al. (2018). Historical (1750–2014) anthropogenic emissions of reactive gases and aerosols from the Community Emissions Data System (CEDS). *Geosci. Model Dev.* 11, 369–408. doi:10.5194/gmd-11-369-2018.
- Joos, F., Roth, R., Fuglestvedt, J. S., Peters, G. P., Enting, I. G., von Bloh, W., et al. (2013). Carbon dioxide and climate impulse response functions for the computation of greenhouse gas metrics: a multi-model analysis. *Atmos. Chem. Phys.* 13, 2793–2825. doi:10.5194/acp-13-2793-2013.
- Karagulian, F., Van Dingenen, R., Belis, C. A., Janssens-Maenhout, G., Crippa, M., Guizzardi, D., et al. (2016). Attribution of anthropogenic PM_{2.5} to emission sources: A global analysis of source-receptor model results and measured source-apportionment data (No. EUR 28510 EN), JRC Technical Reports. Ispra.
- Kühn, T., Kupiainen, K., Mäkinen, T., Kokkola, H., Paunu, V.-V., Laakso, A., et al. (2020). Effects of black carbon mitigation on Arctic climate. *Atmos. Chem. Phys.* 20, 5527–5546. doi:10.5194/acp-20-5527-2020.
- Lee, D. S., Fahey, D. W., Skowron, A., Allen, M. R., Burkhardt, U., Chen, Q., et al. (2020). The contribution of global aviation to anthropogenic climate forcing for 2000 to 2018. *Atmos. Environ.*, 117834. doi:10.1016/j.atmosenv.2020.117834.
- Lund, M. T., Aamaas, B., Stjern, C. W., Klimont, Z., Berntsen, T. K., and Samset, B. H. (2020). A continued role of Short-Lived Climate Forcers under the Shared Socioeconomic Pathways. *Earth Syst. Dyn.* 11, 977–993. doi:10.5194/esd-11-977-2020.
- Markandya, A., Sampedro, J., Smith, S. J., Van Dingenen, R., Pizarro-Irizar, C., Arto, I., et al. (2018). Health co-benefits from air pollution and mitigation costs of the Paris Agreement: a modelling study. *Lancet Planet. Heal.* 2, e126–e133. doi:10.1016/S2542-5196(18)30029-9.
- Purohit, P., Höglund-Isaksson, L., Dulac, J., Shah, N., Wei, M., Rafaj, P., et al. (2020). Electricity savings and greenhouse gas emission reductions from global phase-down of hydrofluorocarbons. *Atmos. Chem. Phys.* 20, 11305–11327. doi:10.5194/acp-20-11305-2020.
- Rao, S., Klimont, Z., Smith, S. J., Van Dingenen, R., Dentener, F., Bouwman, L., et al. (2017). Future air pollution in the Shared Socio-economic Pathways. *Glob. Environ. Chang.* 42, 346–358. doi:10.1016/j.gloenvcha.2016.05.012.
- Rauner, S., Bauer, N., Dirnachner, A., Dingenen, R. Van, Mutel, C., and Luderer, G. (2020). Coal-exit health and environmental damage reductions outweigh economic impacts. *Nat. Clim. Chang.* 10, 308–312. doi:10.1038/s41558-020-0728-x.
- Shine, K. P., Fuglestvedt, J. S., Hailemariam, K., and Stuber, N. (2005). Alternatives to the Global Warming Potential for Comparing Climate Impacts of Emissions of Greenhouse Gases. *Clim. Change* 68, 281–302. doi:10.1007/s10584-005-1146-9.

- 1 Stevenson, D. S., Young, P. J., Naik, V., Lamarque, J.-F., Shindell, D. T., Voulgarakis, A., et al. (2013). Tropospheric
2 ozone changes, radiative forcing and attribution to emissions in the Atmospheric Chemistry and Climate Model
3 Intercomparison Project (ACCMIP). *Atmos. Chem. Phys.* 13, 3063–3085. doi:10.5194/acp-13-3063-2013.
- 4 Thornhill, G. D., Collins, W. J., Kramer, R. J., Olivié, D., Skeie, R. B., O'Connor, F. M., et al. (2021). Effective
5 radiative forcing from emissions of reactive gases and aerosols – a multi-model comparison. *Atmos. Chem. Phys.*
6 21, 853–874. doi:10.5194/acp-21-853-2021.
- 7 Van Dingenen, R., Dentener, F., Crippa, M., Leitao, J., Marmer, E., Rao, S., et al. (2018). TM5-FASST: a global
8 atmospheric source--receptor model for rapid impact analysis of emission changes on air quality and short-lived
9 climate pollutants. *Atmos. Chem. Phys.* 18, 16173–16211. doi:10.5194/acp-18-16173-2018.
- 10 van Marle, M. J. E., Kloster, S., Magi, B. I., Marlon, J. R., Daniau, A.-L., Field, R. D., et al. (2017). Historic global
11 biomass burning emissions for CMIP6 (BB4CMIP) based on merging satellite observations with proxies and fire
12 models (1750–2015). *Geosci. Model Dev.* 10, 3329–3357. doi:10.5194/gmd-10-3329-2017.
- 13 Vandyck, T., Keramidas, K., Tchung-Ming, S., Weitzel, M., and Van Dingenen, R. (2020). Quantifying air quality co-
14 benefits of climate policy across sectors and regions. *Clim. Change* 163, 1501–1517. doi:10.1007/s10584-020-
15 02685-7.
- 16
- 17

ACCEPTED SUBJECT TO FINAL EDITING